

Coherent Coastal Sea-Level Variability at Interdecadal and Interannual Scales from Tide Gauges

Authors: Papadopoulos, A., and Tsimplis, M. N.

Source: Journal of Coastal Research, 2006(223) : 625-639

Published By: Coastal Education and Research Foundation

URL: <https://doi.org/10.2112/04-0156.1>

BioOne Complete (complete.BioOne.org) is a full-text database of 200 subscribed and open-access titles in the biological, ecological, and environmental sciences published by nonprofit societies, associations, museums, institutions, and presses.

Your use of this PDF, the BioOne Complete website, and all posted and associated content indicates your acceptance of BioOne's Terms of Use, available at www.bioone.org/terms-of-use.

Usage of BioOne Complete content is strictly limited to personal, educational, and non - commercial use. Commercial inquiries or rights and permissions requests should be directed to the individual publisher as copyright holder.

BioOne sees sustainable scholarly publishing as an inherently collaborative enterprise connecting authors, nonprofit publishers, academic institutions, research libraries, and research funders in the common goal of maximizing access to critical research.

Coherent Coastal Sea-Level Variability at Interdecadal and Interannual Scales from Tide Gauges

A. Papadopoulos[†] and M.N. Tsimplis[‡]

[†]Mineral Resources
Engineering Department
Technical University of Crete
73 100, Chania, Greece
tpapadop@mred.tuc.gr

[‡]James Rennell Division for
Ocean Circulation and
Climate
Southampton Oceanography
Centre
Empress Dock
Southampton, Hants SO14
3ZH, United Kingdom
mnt@soc.soton.ac.uk

ABSTRACT



PAPADOPOULOS, A. and TSIMPLIS, M.N., 2006. Coherent coastal sea-level variability at interdecadal and interannual scales from tide gauges. *Journal of Coastal Research*, 22(3), 625–639. West Palm Beach (Florida), ISSN 0749-0208.

Coastal sea level measured from tide gauges exhibits coherent variability at interannual and decadal scales. We investigate sea-level variability of large geographic areas using annual mean sea-level values obtained from the longest available records of coastal observations. Eight sea-level regional indices are constructed for the Atlantic and the Pacific Ocean basins. High coherency of sea-level variability at the decadal timescales between different oceanic regions is observed. The role of large-scale atmospheric forcing is then examined by comparison with the El Niño–Southern Oscillation (ENSO) and the North Atlantic Oscillation (NAO). Strong correlation between the NAO and the second empirical orthogonal function (EOF) of the northwest Atlantic data set was observed. The second EOF is also significantly correlated with the latitudinal position of Gulf Stream and the Arctic Oscillation (AO). Sea-level changes in the northeast Atlantic are driven by the NAO. Correlation with the AO was also observed. In the Pacific Ocean, ENSO dominates sea-level variability along the eastern and southwest sides of the basin. ENSO signatures appear also in the southwest Atlantic, indicating teleconnection patterns. It is proposed that ENSO-related variability in this region is forced through the Pacific–South American teleconnection mechanism. The correlation between southwest Atlantic sea level and ENSO increased after 1980. Sea-level variability on decadal scales in the northwest Pacific region is influenced by the Pacific Decadal Oscillation.

ADDITIONAL INDEX WORDS: Teleconnections, indices, regional sea level, North Atlantic Oscillation, El Niño–Southern Oscillation, Southern Oscillation Index, Arctic Oscillation, Pacific Decadal Oscillation.

INTRODUCTION

Global sea-level rise is a major threat to the coastal environment and is expected to accelerate with global warming (CHURCH *et al.*, 2001). Past measurements of sea level are based on tide-gauge observations that cover more than 150 years. These indicate a value for the global sea-level rise in the range of 1–2 mm/y (CHURCH *et al.*, 2001). Nevertheless, most of these tide gauges are located in the Northern Hemisphere and it has been questioned whether they truly represent the global ocean. CABANES, CAZENAVE, and LE PROVOST (2001) raised further doubts by observing that the thermal expansion in the areas in which these long-term tide gauges are located is faster than the global average. This view is disputed (MILLER and DOUGLAS, 2004; TSIMPLIS and RIXEN, 2002), but nevertheless the spatial bias in the oldest sea-level records is real. Moreover, coastal estimates of sea-level rise are bound to differ to some extent from true global means (HOLGATE and WOODWORTH, 2004).

Sea-level measurements from tide gauges are relative to land. The separation of the land movement from the sea-level signal cannot be made without additional independent measurements (see for example WOODWORTH, 1990). Nevertheless, within the context of climate change one can focus on regionally coherent signals extracted from groups of tide gauges and consider all the residuals as local land movement or local oceanic variability. The coherent signals will contain the mean oceanic changes and mean land movement. If detrended sea-level data are used, the mean oceanic and land movement component can be assumed very small. Thus regional sea-level indices can be developed to improve the understanding of the role of regional- or global-scale forcing to regional coastal sea level.

Sea-level indices as well as empirical orthogonal functions (EOFs) of sea level have been in use for a long time, and numerous studies based on this methodology exist. WOODWORTH (1990) summarises their advantages and disadvantages and supports the development of such indices as a higher-order product of the otherwise localised sea-level measurements that can provide “at-a-glance” information of the sea-

DOI:10.2112/04-0156.1 received 21 January 2004; accepted 7 April 2004.

level behavior in a region. SHENNAN and WOODWORTH (1992) and later WOODWORTH *et al.* (1999) have produced sea-level indices for the UK. Other examples range from the correlation of the strength of the Pacific Ocean equatorial current system to sea-level indices (WYRTKI, 1974; these are routinely used to describe the strength of equatorial currents and countercurrents <http://www.soest.hawaii.edu/UHSLC/>) to the combination of short fragmented sea-level records in the Eastern Mediterranean to develop a long-term reliable sea-level index (TSIMPLIS and JOSEY, 2001).

In this study the regional sea-level indices developed are compared with regional climatic indices to obtain a better understanding of the mechanisms that can affect future sea-level changes on regional scales. The aim is to resolve the spatial domain and the frequency domain at which climatic indices affect sea level.

In the North Atlantic, the most prominent atmospheric oscillation pattern is the North Atlantic Oscillation (NAO). The NAO index is defined as the standardised sea-level atmospheric pressure differences between the Icelandic Low and the Azores High. During the last decades, an increasing trend in the winter values of NAO has been observed (HURRELL, 1995, 1996; JONES, JÓNSSON, and WHEELER, 1997). Interactions between NAO and climatic change are still not well understood (ZORITA and GONZALES-ROUCO, 2000), but the recent changes in NAO may be linked to climate change (CORTI, MOLteni, and PALMER, 1999; HURRELL, 1995; OSBORN *et al.*, 1999; SHINDELL *et al.*, 1999). Another atmospheric oscillation in the region is the Arctic Oscillation (AO) (THOMPSON and WALLACE, 1998), but this pattern is very similar to NAO (WALLACE, 2000).

The effects of NAO on sea level for the regions of the north-west European continental shelf and the Baltic and Mediterranean Seas have been the subject of recent studies (TSIMPLIS and JOSEY, 2001; TSIMPLIS *et al.*, 2004; WAKELIN *et al.*, 2003; WOOLF, SHAW, and TSIMPLIS, 2004; YAN, TSIMPLIS, and WOOLF, 2004). In the North Sea, correlation of NAO with sea level has been observed throughout the 20th century, but this influence has been stronger during the last 20 years. Sensitivity of sea level in the region varies from positive to negative values for the northeast to the south of the region respectively (WAKELIN *et al.*, 2003). Similarly in the Baltic, winter mean sea-level values were found to correlate with NAO index since the 19th century. This correlation has been stronger in the 20th century and even more intense during the last 20 years (ANDERSSON, 2002). In both regions sea level appears to respond to changes in the westerly winds associated with NAO, rather than directly to sea-level pressure (SLP) changes. In the Mediterranean Sea, NAO forcing is associated with combined effects of atmospheric pressure anomalies and changes in evaporation–precipitation balance (TSIMPLIS and JOSEY, 2001). Steric sea-level changes in the upper layers of the Adriatic and Aegean Seas are also correlated with NAO (TSIMPLIS and RIXEN, 2002).

Sea-level variability in the tropical Pacific is dominated by the El Niño Southern Oscillation (ENSO). The weakening of the southeast trades during ENSO allows warm water masses from the west tropical Pacific to propagate eastward as Kelvin waves reach the coast of Peru about 2 months after

the weakening of the trades (CHELTON and ENFIELD, 1986). There, they get deflected and split into two waves that travel toward the South and the North Poles respectively. In contrast, in the southwest side of the basin the occurrence of ENSO leads to lowering of water as warm water masses are transported toward the east. Nevertheless ENSO events are not only important in the Pacific. CAZENAVE *et al.* (1998) and NEREM *et al.* (1999) illustrate how global sea surface temperature (SST) and global mean sea level obtained from satellite altimetry respond to major ENSO events. In addition, numerous teleconnections with the ENSO in observations and models have been extensively reported in the scientific literature for all the oceanic basins.

Thus, for example, teleconnections in pressure and rainfall with the extra-tropical Pacific region have been claimed (see for example CHOU, TU, and YU, 2003). In addition, correlation of the ENSO with the tropical Atlantic SSTs (see for example GIANNINI *et al.*, 2001) with the Sahel rainfall (JANICOT, TRZASKA, and POCCARD, 2001) and the Indian Ocean are also documented (see for example ALLAN *et al.*, 2003). The Pacific–South American (PSA) teleconnection pattern (CARLETON, 2003; GARREAU and BATTISTI, 1999; KAROLY, 1989; MO and HIGGINS, 1998) manifests itself as a barotropic standing wave of atmospheric pressure anomalies from Australia into South America and the southwest Atlantic at seasonal and interannual scales. Changes in atmospheric pressure and SST linked to ENSO can affect sea level (CAZENAVE *et al.*, 1998). In addition, precipitation changes lead to river outflow variations that are reflected in sea-level measurements from tide gauges located at the river mouths. For example, DOUGLAS (2001) discusses the effect of ENSO on South American rainfall, which affects runoff in the River Plate. In the North Pacific, the Pacific Decadal Oscillation (PDO) (*e.g.*, HARE, MANTUA, and FRANCIS, 1999; ZHANG, WALLACE, and BATTISTI, 1997) is also a climate pattern related to SLP and SST variability. PDO strongly related with ENSO and it can be referred to as ENSO-like interdecadal variability (ZHANG, WALLACE, and BATTISTI, 1997).

In this work we construct reference series to describe coherent sea-level changes over large geographic areas on interannual timescales. We explore the correlation of the ENSO and NAO indices to the derived regional sea-level time series and we search for teleconnections between the regional indices and the NAO and Southern Oscillation Index (SOI). We also investigate for correlation between the regional sea-level indices and other climate indices that are related to NAO and ENSO, namely the AO and the PDO.

DATA AND METHODOLOGY

Annual mean sea levels from tide-gauge records were obtained from the Permanent Service for Mean Sea Level (PSMSL) (WOODWORTH and PLAYER, 2003). The PSMSL database includes in excess of 2000 stations of variable duration and data quality. For this study the following criteria were observed. Only stations with at least 30 years of revised local reference data were selected. Stations less than 95% complete were omitted in the Northern Hemisphere where there is an abundance of data. Nevertheless, in the Southern Hemisphere,

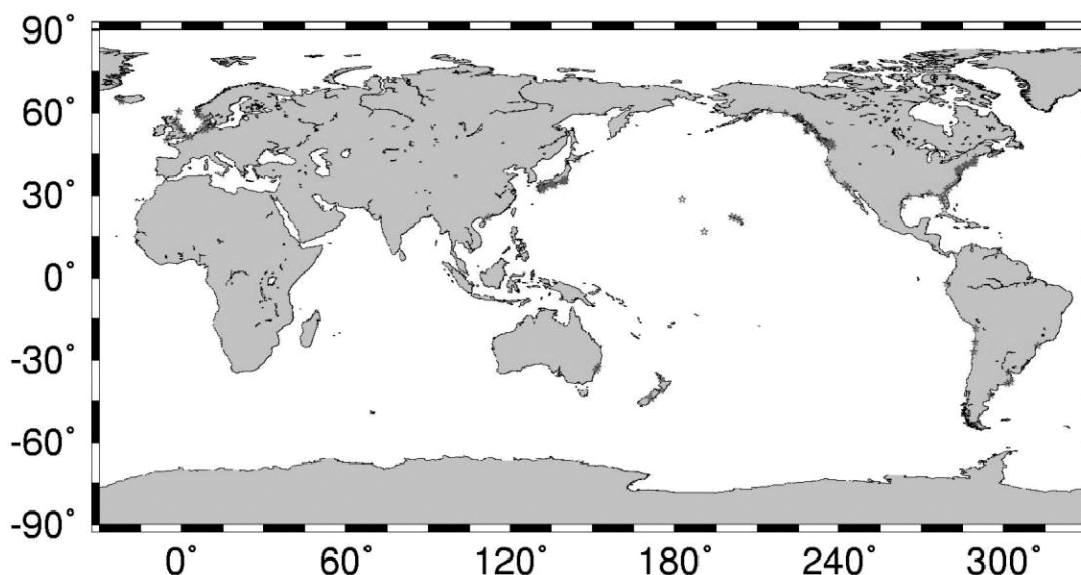


Figure 1. The geographical location of the tide gauges, indicated as dots, that were used in the analysis.

where not many long records exist, stations less than 95% complete were also used. Stations with suspect data or suspect datum history or stations with gaps larger than 5 years or stations in semiencloded seas (for example the Mediterranean and the Baltic) or affected by rivers were also excluded.

The resulting 98 stations used in the analysis were grouped into eight groups according to their geographical location (Figure 1). Thus, in the Atlantic Ocean (Figure 2) one index was constructed for the northeast Atlantic and North Sea, while two more indices were constructed for the north and south parts of the western side of the basin. Similarly, two indices were constructed in the South Pacific for the eastern and western sides respectively, and three indices in the North Pacific for the eastern, central, and western parts of the basin (Figure 3). Linear trends were removed from the time series. Because the length of the time series varies, the calculation of trend was done over the period for which each regional sea-level index was calculated rather than for each whole record. Thus within each region any errors in the estimation of the trend due to decadal variability will, at least, be consistent within the regional sets of stations.

Gaps in the time series were filled by regressing that particular time series on the nearest tide-gauge records for the periods they all have data and then using the regression coefficients to estimate the missing values. Where the spatial distribution within a group was not uniform, *i.e.*, there were areas of higher density of stations; the data from these stations were averaged until spatial uniformity was obtained. Thus the number of time series was reduced to 50. In each of the eight regions, the EOFs of the time series were extracted (see for example PREISENDORFER, 1988). To avoid any biases toward stations with higher variability, all data were standardized (*i.e.*, time series were scaled to have unit variance) before the EOF extraction.

To distinguish between statistically significant EOFs and noise, the bootstrap method was used. Data from all n stations within a region were randomly shuffled and then the EOFs were extracted. This procedure was repeated 1000 times, and each time the explained variance of the k th EOF ($1 \leq k \leq n$) of the shuffled time series was compared with the explained variance of the k th EOF of the data being analyzed. The k th EOF was considered statistically significant if at least in 95% of these comparisons the variance it explained was higher than the corresponding EOF of the shuffled time series.

For example, the results for northeast Atlantic (Figure 4) indicate that for this region only the first EOF is significant. Indeed in half of the regions only the first EOF was significant. In these cases, this first EOF was considered to be the regional sea-level index. In the regions where the second EOF was significant, the index was constructed by adding the first and second EOFs. Third or higher EOFs were never used in the construction of the indices, but have been used in the discussion of the southwest Atlantic region.

To perform the EOF analysis, the data from different stations must cover the same period and also have zero mean during that epoch. Because some records contain more data than others, the data over common periods were used to extract 'partial' sea-level indices. But the longer records in the data set that are used for the creation of more than one partial index will not have zero mean during the period covered by each partial index. Thus the average value of the data used to create a partial index was then added to that partial index, before connecting the partial indices to create the regional index.

As an example of the procedure, Figure 2b demonstrates how the index for the northeast Atlantic was created. Fifteen time series were found to satisfy the criteria mentioned

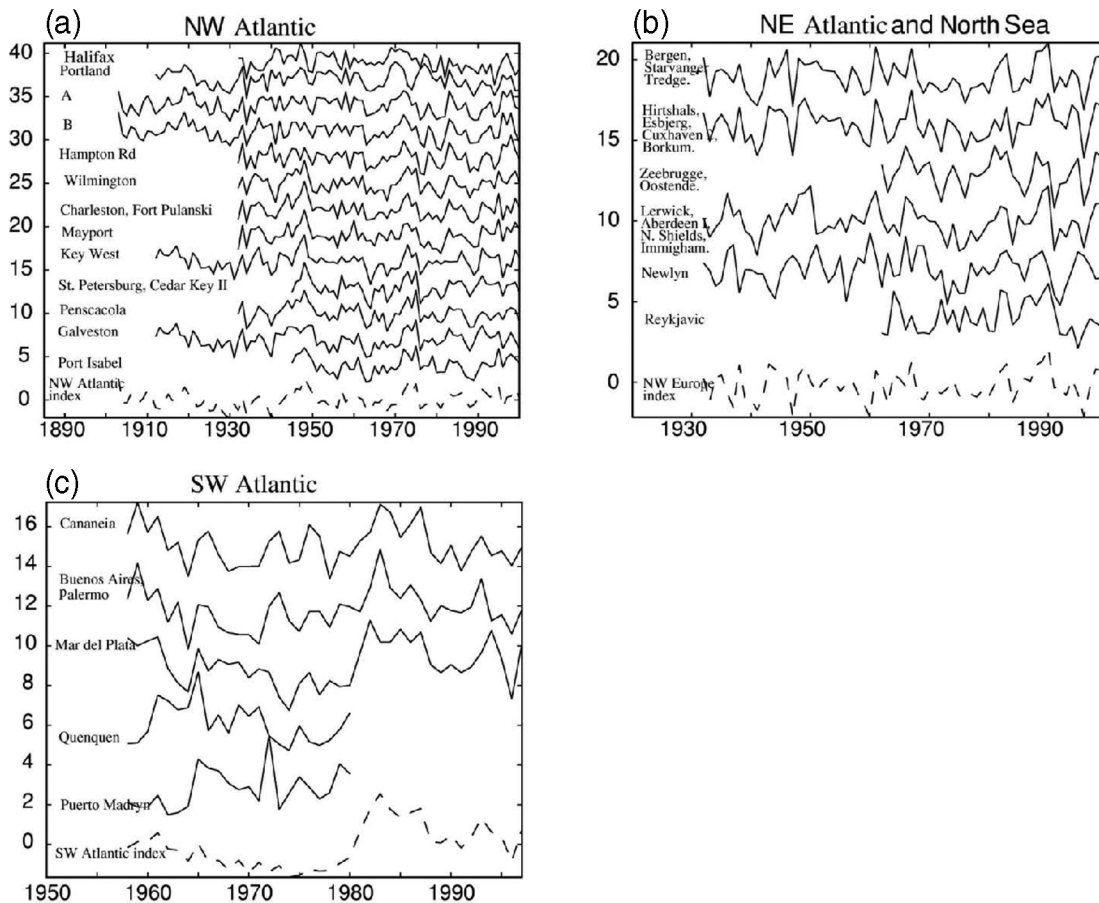


Figure 2. The tide-gauge records (detrended, missing values filled) used in the construction of the three indices for the Atlantic Ocean (dashed lines). From top left and moving clockwise, northwest Atlantic index (a), northeast Atlantic and North Sea index (b), and southwest Atlantic index (c).

above. After detrending and filling any gaps in the data, some of the series were averaged to obtain spatial uniformity. The names of the stations averaged appear at the left of the time series. Six (standardized) time series are indicated with solid curves, four of which correspond to the period 1932–2000, whereas the other two correspond to the period 1962–2000. Two different partial indices were thus created covering the epochs 1932–61 and 1962–2000 respectively. The four series that cover both of these epochs have zero mean for the period 1932–2000, but do exhibit zero mean in either of the periods 1932–61 or 1962–2000. For example, detrended and standardized sea-level data from Newlyn has -0.0363 mean value for the epoch 1932–61, and 0.0214 for the period 1961–2000. But the data series were forced to have zero mean in both epochs to extract the EOFs. Thus, the regional index was generated by adding the mean value of the data to the partial indices before merging the partial indices into one series. If one had just connected the two partial indices, there would have been an artificial step in the regional index between 1961 and 1962.

The resulting regional indices represent sea levels but they are dimensionless and do not represent the true sea-level variability, as the data used were standardized before the EOF

extraction. The standardized time series from which the indices were created can be found in Figures 2 and 3 for the Atlantic and Pacific Basins respectively. The explained data variance of the EOFs used in the analysis and the weights (principal component coefficients) of each station are tabulated in the Appendix.

The significance of the correlation coefficient was also based on the bootstrap method. All the correlation coefficients mentioned in the discussion as significant exhibit confidence intervals higher than 95%. The next section focuses on the description of the sea-level indices. It provides a comparison amongst the indices for the identification of similarities and correlation of the observed signals. A search for the signature of major events, teleconnections, and dominant forcing mechanisms is also presented.

Several indices are available to describe the ENSO (HANLEY *et al.*, 2003). Some are based on regional SST indices, some on atmospheric pressure differences, and some on combinations of environmental parameters (HANLEY *et al.*, 2003). Atmospheric pressure differences have long been used as an index usually referred to as the Southern Oscillation Index (SOI) (HOREL and WALLACE, 1981). For this study the SOI was obtained from the Climate Prediction Center (CPC) website (<http://www.cpc.ncep>).

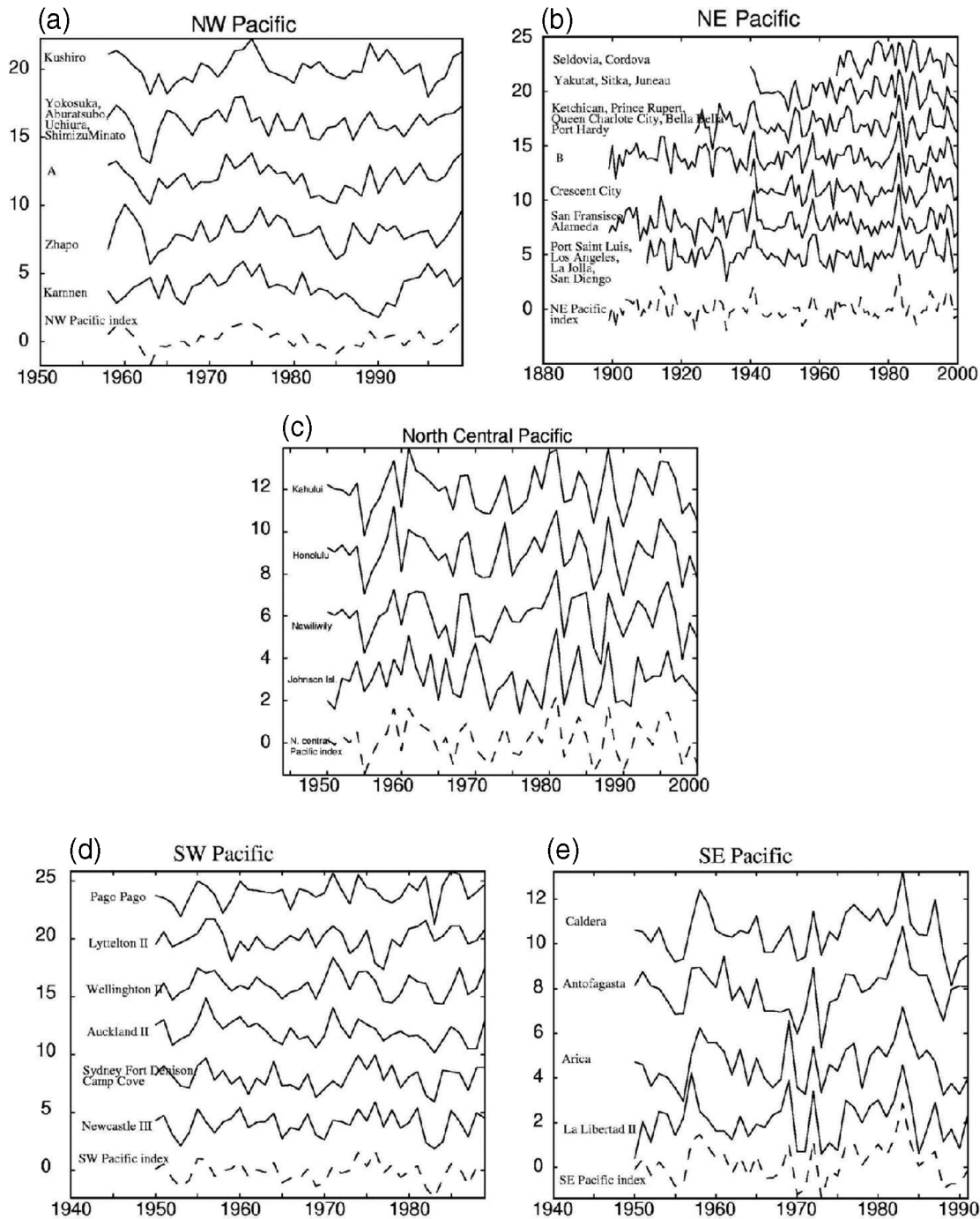


Figure 3. The tide-gauge records (detrended, missing values filled) used in the construction of the five indices for the Pacific Ocean (dashed lines). From top left and moving clockwise, northwest Pacific index (a), northeast Pacific index (b), north-central Pacific index (c), southwest Pacific index (d), and southeast Pacific index (e).

noaa.gov/data/indices/index.html) and is defined as standardized sea-level pressure differences between Tahiti and Darwin. A positive value of the SOI pressure index is indicative of strong South Pacific trade wind circulation and equatorial westerlies. The pressure difference SOI index is strongly (negatively) cor-

related with the SST-based indices (see for example HANLEY *et al.*, 2003; HOREL and WALLACE, 1981). The latitudinal position of the Gulf Stream North Wall index was obtained from the Plymouth Marine Laboratory (<http://www.pml.ac.uk/gulfstream/>). The NAO index used in the analysis is the average winter

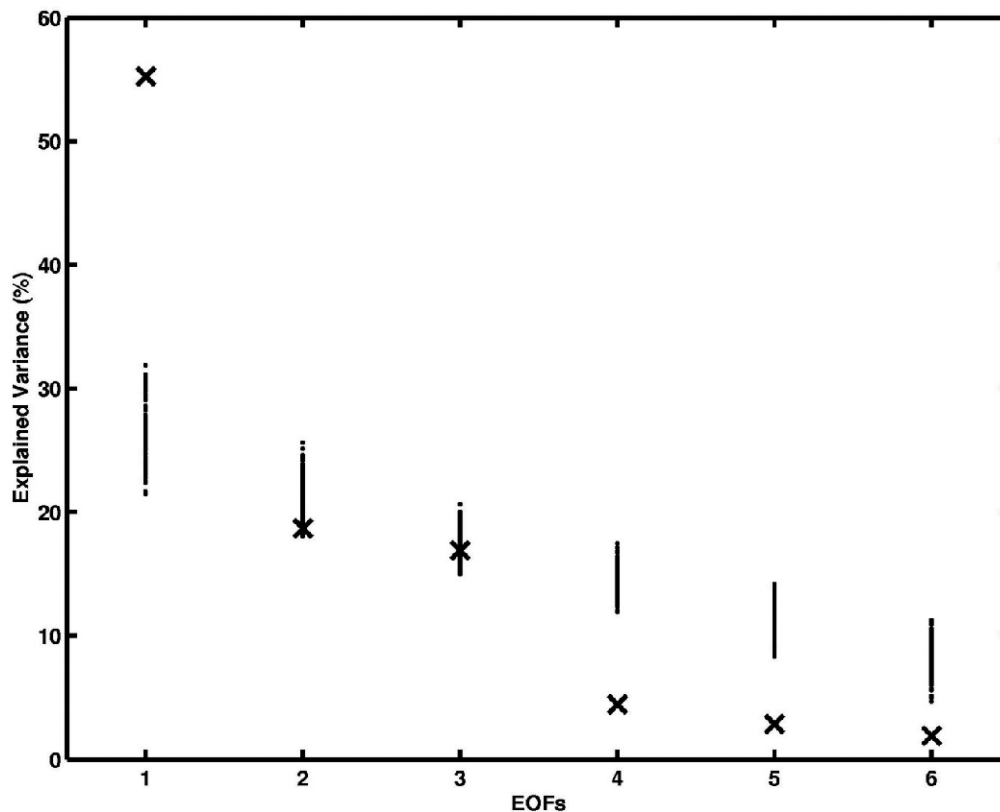


Figure 4. Bootstrap method indicates that in the northeast Atlantic and North Sea index, only the first empirical orthogonal function (EOF) is statistically significant. Dots represent the variance explained by the associated EOF of the shuffled series, whereas 'x' marks stand for the explained variance of the original tide-gauge records.

NAO index (December–March) calculated from data from JONES, JÓNSSON, and WHEELER (1997). The PDO index was obtained from the Joint Institute for the Study of the Ocean and the Atmosphere (<http://jisao.washington.edu/pdo/PDO.latest>), and represents the leading EOF of the November-to-March SST anomalies in the Pacific Ocean to the North of 20°N. The AO index used is the winter mean AO (December–March) obtained from the CPC website (http://www.cpc.ncep.noaa.gov/products/precip/CWlink/daily_ao_index/ao_index.html).

There are other climatic indices that can be used. Nevertheless, most of them, like the PDO in the northern Pacific Basin, or the AO in the northern Atlantic, are not independent from the two major ones, namely the SOI and the NAO indices, which have been found to represent the main modes of climate variability of the atmosphere–ocean system.

RESULTS AND DISCUSSION

Atlantic Ocean

Sea level in the northwest Atlantic appears to slowly decrease from the beginning of the century until about 1940 (Figure 2a). Of course this decrease, like the rest of variability described in this section, is relative to the long-term trend

that was removed from the data set before the construction of the indices. At that point there is a rapid increase that lasts about 10 years and after that sea level drops again until the mid-1960s. From the late 1960s until 2000 a small but positive trend can be detected. During the late 1960s an increase of sea level is also evident in the northeast Atlantic (Figure 2b). This increase lasts until the early 1990s. Before this period no other slow changes in the mean can be detected in the northeast Atlantic. In the southern Atlantic the only reliable data come from the western side of the basin. Sea level in the region of southwest Atlantic (Figure 2c) decreases from the early 1960s until the early 1970s and then increases for a few years. A steady decrease initiates in the early 1980s and lasts until the end of the index in 1997.

The region where the tide gauges used for the construction of the northeast Atlantic index are sited is affected by NAO. Figure 5 demonstrates how sea-level changes in this region are correlated to winter NAO (JONES, JÓNSSON, and WHEELER, 1997). The correlation coefficient for the period (1932–1997) is 0.65, which is statistically significant. It should be noted that the second EOF of the data has also been used in this comparison, although bootstrap indicates that this EOF is not statistically significant. Significant correlation, 0.49, was also observed between the northeast Atlantic sea-level index and the AO index.

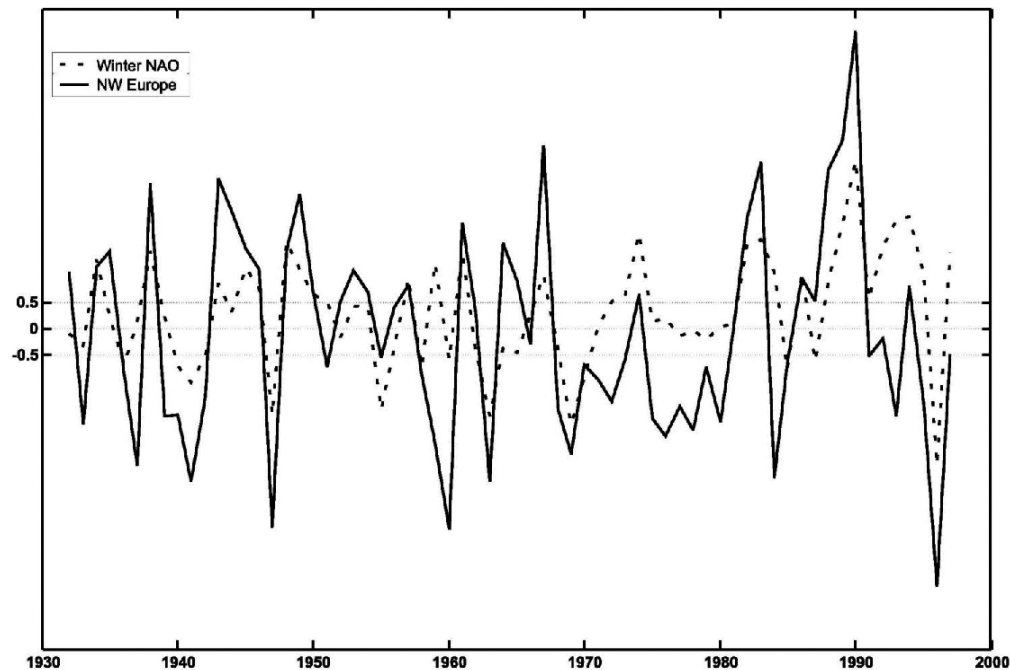


Figure 5. Correlation coefficient of winter North Atlantic Oscillation (dashed line) with northwest Europe index (solid line). Both the first and second empirical orthogonal functions of the tide-gauge data have been used in the comparison.

Although the northwest Atlantic is also influenced by NAO, there is no correlation between the NAO and the northwest Atlantic indices. Such a result is expected, as only half of the tide-gauge stations used lie within the region where NAO is active. Thus, one should search for an NAO signature on the second EOF of the data. The second EOF of the northwest Atlantic index exhibits significant (0.54) correlation coefficient with the winter NAO Jones index (Figure 6). Similarly, this second EOF exhibits correlation coefficient 0.47 with the AO index. Figure 7 illustrates that the second EOF of this sea-level regional index is also correlated with the latitude of the north wall of the Gulf Stream index (correlation coefficient 0.56). The latitude of Gulf Stream and winter NAO series used exhibit 0.30 correlation, which increases to 0.65 when NAO lags 1 year and reaches 0.69 when NAO lags 2 years. The latitude of Gulf Stream derived from Topex/Poseidon shifts northward (southward) 11–18 months after NAO reaches positive (negative) extrema (SIRVEN *et al.*, 2002).

Pacific Ocean

Similarly to the Atlantic basin, both interannual and lower-frequency changes can be detected in the Pacific. In the northeast side of the basin (Figure 3b), sea level increases from the beginning of the century until about 1915 and then decreases until the mid-1920s. Another sea-level increase initiates in the early 1970s and holds until today. In the southeast Pacific (Figure 3e), sea level drops from mid-1950s for about 10 years and then rises again until about 1982. Another decrease of sea level occurs also in the mid-1950s in the

southwest Pacific (Figure 3d) and lasts until the late 1960s. Sea level then rises again for the next 10 years. In the northwest side (Figure 3a) of the basin interdecadal variability is more enhanced in comparison with the other areas. There, sea level increases from the early 1960s for about 15 years and then drops for another 10. After 1985, sea level increases again until the end of the period covered by the index. No significant slow changes of sea level in north-central Pacific (Figure 3c) were observed.

As expected, the most prominent feature in the Pacific is the effect of ENSO. ENSO dominates the sea-level forcing in the interannual frequencies in the northeast side of the basin, as well as in either sides of the southern Pacific (Figure 8). Table 1 contains the correlation coefficients amongst the sea-level indices, which showed statistically significant correlation with the SOI. The Eastern coast is negatively correlated with the southwest coast as well as with SOI, whereas the southwest part of the basin exhibits strong positive correlation with SOI. Thus, El Niño (La Niña) events can be identified as local sea-level maxima (minima) along the eastern coast and as minima (maxima) in the southwest part of the basin, and vice versa in the indices of the eastern Pacific.

The common interannual variability along the eastern coast is due to coastal trapped Kelvin waves that move poleward along (CHELTON and DAVIS, 1982; CHELTON and ENFIELD, 1986). It has also been proposed (BYE and GORDON, 1982) that the common sea-level variability between the eastern and southwest Pacific is linked with fluctuations in the intensity of the subtropical oceanic gyres.

In northwest Pacific, the regional sea-level index is anti-

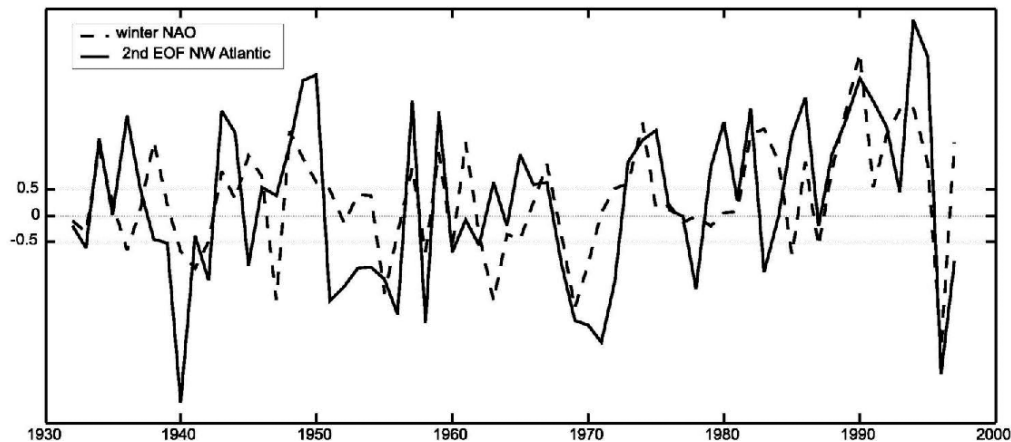


Figure 6. Winter North Atlantic Oscillation (dashed line) coplotted with the second empirical orthogonal function of northwest Atlantic tide-gauge records (solid line).

correlated on decadal scales with PDO (Figure 9). The associated correlation coefficient is -0.59 for the period after 1970. This may result from steric forcing, as the positive phases of PDO are linked with negative SST anomalies in the region (MANTUA *et al.*, 1997). Cross-correlation of the first and second EOFs of the sea-level data of northwest Pa-

cific and their sum (*i.e.*, the regional index) with the indices obtained for the southwest, northeast, southeast, and north-central Pacific did not give any statistically significant results. Similarly, no correlation was observed between north-central Pacific and any other regional index or the SOI and PDO indices. This is inconsistent with the results of WANG,

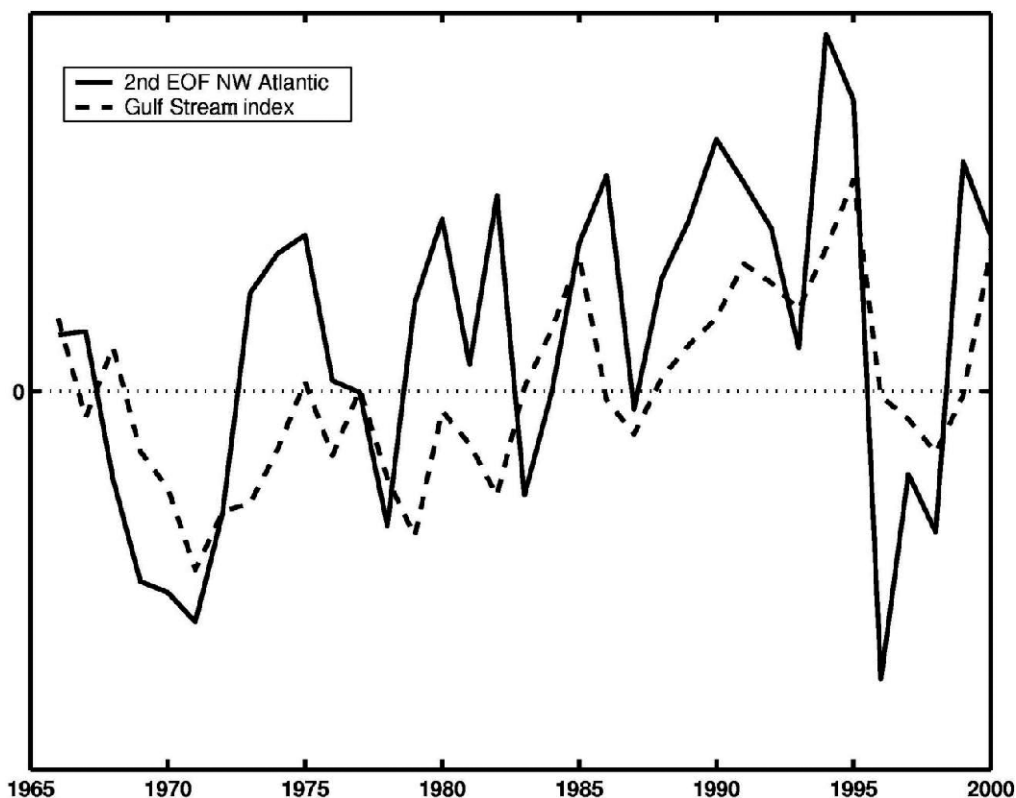


Figure 7. The second empirical orthogonal function of northwest Atlantic (solid line) data set coplotted with the latitudinal position of the Gulf Stream index (dashed curve).

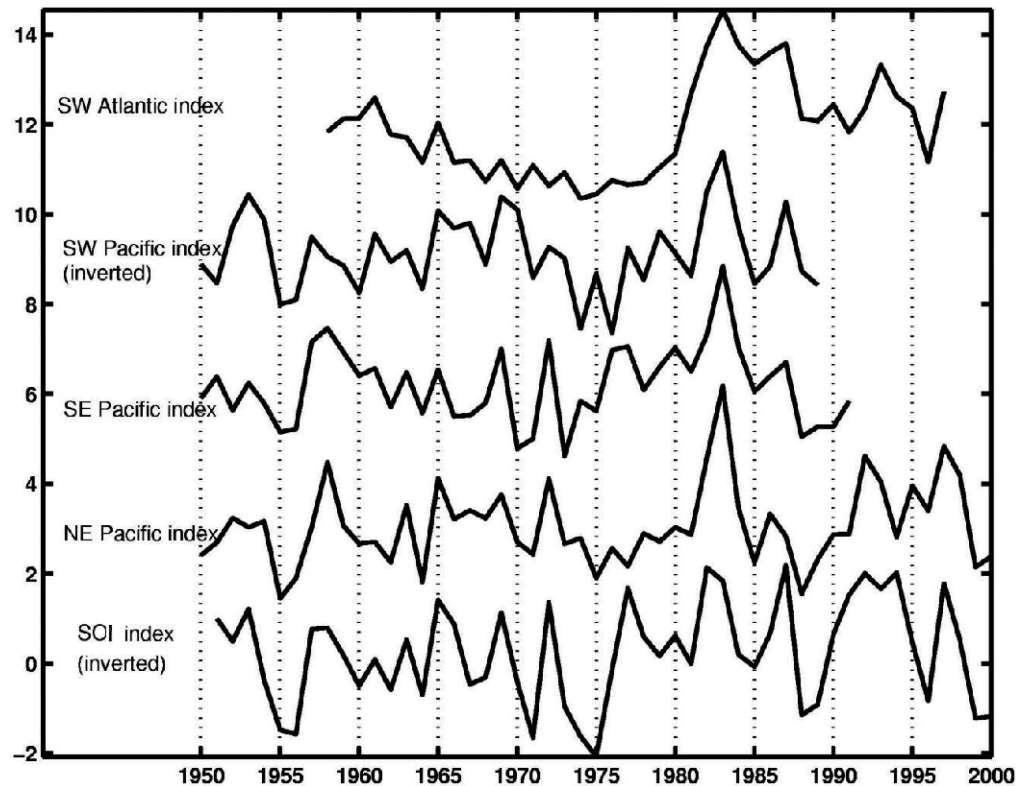


Figure 8. The four regional indices that correlate with the Southern Oscillation Index (SOI). Starting from the top, southwest Atlantic, southwest Pacific, southeast Pacific, northeast Pacific, and SOI. Note that for illustration purposes, southwest Pacific and SOI indices are inverted.

Wu, and Fu (2000), who showed that, during the peaking of El Niño and La Niña episodes, there are statistically significant differences in SLP anomalies and surface wind anomalies in the regions described by the northwest and north-central Pacific indices. The discrepancy is probably due to the fact that WANG, WU, and FU (2000) used 3-month composite anomalies during the mature stages of extreme phases of the ENSO, whereas this work is based on the analysis of annual means.

Many of the stations used for the construction of the northwest and north-central Pacific regional indices are sited in the vicinity of the Kuroshio. HWANG and KAO (2002), using altimetric data from Topex/Poseidon, discovered strong correlation between ENSO and volume transport of Kuroshio northeast of Taiwan with a month lag, and strong negative correlation between ENSO and both volume transport and velocity of Kuroshio southeast of Taiwan with 9–10 months

lead respectively. Such correlation was not observed with either of our two indices, as none of the tide gauges used in the analysis is close to Taiwan. Some of the stations used in the present analysis were also used by BLAHA and REED (1982) to study variability in the flow of the Kuroshio Current; they also inferred that most of the interannual fluctuations in Kuroshio are not associated with ENSO.

The flow of Kuroshio extension current affects most of the stations of the northwest Pacific index. QIU (2000) proposes that interannual variations in the Kuroshio extension system can be regionally or remotely forced by surface wind and buoyancy forcing over the North Pacific. These variations could also result from internal ocean dynamics associated with the Kuroshio's southern recirculation gyre variability. QIU (2000) concludes that further studies are needed to clarify the causes and dynamics of such physical processes.

Teleconnections

Comparison of the sea-level indices constructed for the Pacific Ocean with the southwest Atlantic index (Figure 8) reveals that ENSO forcing is also present in southwest Atlantic. This region exhibits -0.50 correlation with the SOI for the period 1958–97. The two signals are in phase except in the years 1973, 1981, and 1991. This establishes a teleconnection between the southwest Atlantic and the regions of the

Table 1. Correlation coefficients amongst the four indices that were correlated with Southern Oscillation Index (SOI).

| | NE Pacific | SW Pacific | SE Pacific | SW Atlantic |
|------------|------------|------------|------------|-------------|
| SOI | -0.64 | 0.66 | -0.73 | -0.50 |
| NE Pacific | | -0.66 | 0.69 | 0.44 |
| SW Pacific | | | -0.40 | -0.44 |
| SE Pacific | | | | 0.40 |

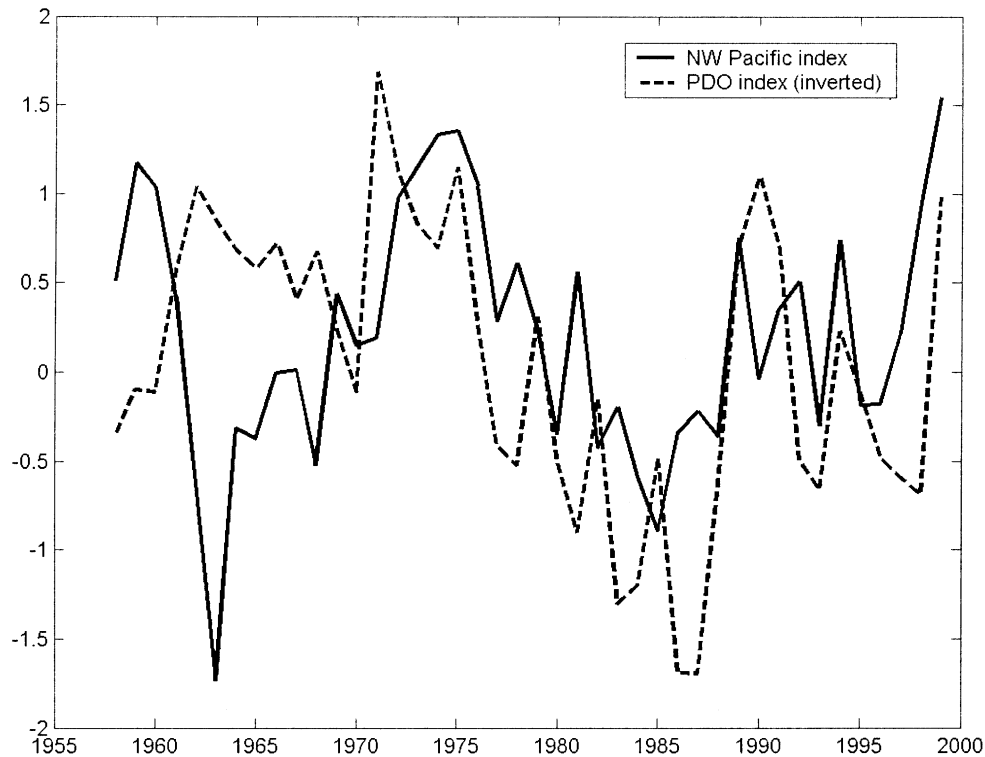


Figure 9. The northwest Pacific regional sea-level index (solid line) together with the inverted Pacific Decadal Oscillation index (dashed line).

Pacific that correlate with SOI, and demonstrates that ENSO affects sea level also in parts of the Atlantic Ocean.

The observed similarities between the SOI signal and the southwest Atlantic index are likely not of oceanic nature, although the southwest Atlantic and the Southern Pacific are linked via the Southern Ocean (e.g., WHITE and PETERSON, 1996) because the estimated timescale for the transmission are of the order of multiple years (PETERSON and WHITE, 1998). Thus the mechanism that generates signals similar to ENSO in the southwest Atlantic sea-level index must be of atmospheric nature (DOUGLAS, 2001).

ENSO-related variability can be teleconnected along the southwest Atlantic coast through the PSA mechanism through changes in lower atmospheric circulation and SLP along the southeast coast of South America as well as by changes in precipitation (DOUGLAS, 2001). The region where the tide gauges used for the construction of the southwest

Atlantic regional sea-level index are sited is associated with wetter than usual conditions during El Niño years. The exact opposite happens during La Niña years (CPC). Although tide-gauge stations that according to PSMSL are influenced by river output were omitted in this study, two of the stations used (Buenos Aires and Palermo) are sited within Rio de la Plata Bay where the Parana and Uruguay rivers outfall, and Cananea may be affected by nearby estuaries (PSMSL documentation). Thus, the ENSO-related signal in half of the data set used may be partially a result of the precipitation regime discussed above.

But this ENSO-related forcing on sea level along the south-east American coast has not remained the same throughout the period 1958–97. To understand that, one should first consider how this sea-level index was created. This sea-level index was created by merging two different ‘partial indices’ into one series. The first one utilized data from six tide-gauge stations (five usable time series after averaging Palermo and Buenos Aires data) and covered the period between 1958 and 1980, whereas the second was constructed on the basis of data obtained from three tide gauges and covered the time span between 1981 and 1997. Inspection of the correlation coefficients between the tide-gauge series and SOI for these two time spans (Table 2) reveals that there is a significant change on the ENSO-related mechanisms that act in this region. Before 1980 there is no evident ENSO signature on the data of individual tide-gauge series, whereas after 1980 correlation with ENSO is apparent.

Table 2. Correlation coefficients between Southern Oscillation Index and the tide gauge series that were used to construct the southwest Atlantic index for two different time spans, 1958–80 and 1981–97.

| | 1958–80 | 1981–97 |
|---------------|---------|---------|
| Puerto Madryn | −0.35 | No data |
| Quequen | −0.08 | No data |
| Mar Del Plata | −0.26 | −0.62 |
| Buenos Aires | −0.33 | No data |
| Palermo | −0.29 | −0.52 |
| Cananea | −0.17 | −0.48 |

Table 3. During 1958–80, the correlation of Southern Oscillation Index (SOI) with southwest Atlantic index (first empirical orthogonal function [EOF]) increases when the second, third, and fourth EOFs are taken into account. The second column contains the variance of the data explained by the reconstructed series.

| | Variance Explained | Correlation with SOI |
|--------------------------------------|--------------------|----------------------|
| First EOF | 37.5% | −0.26 |
| First + second EOFs | 64.1% | −0.32 |
| First + second + third EOFs | 85.7% | −0.45 |
| First + second + third + fourth EOFs | 95.2% | −0.49 |

For the period 1981–97, the first EOF of the data set explains 64% of the data variance and was the only significant EOF. Correlation coefficient between this first EOF and the SOI is −0.66. When the sum of first and second EOF was compared to the SOI the correlation coefficient decreased, indicating that the entire ENSO-related signal is concentrated in the first EOF of the data.

In the period 1958–1980 the situation is different. As illustrated in Table 3, the first EOF explains only 37.5% of the data variance and the correlation coefficient with the SOI is −0.26. When more EOFs are being taken into account the correlation with SOI increases and reaches −0.49 when the first four EOFs are utilized. It should be noted that Bootstrap test suggests that in this case only the first EOF is statistically significant. Thus, higher EOFs should be treated with caution as they may be contaminated by noise. In the case of 1958–80 partial index, inspection of the EOF weights (see Appendix) indicates that in the extraction of the first EOF, the two southernmost tide gauges (Puerto Madryn and Quen Quen) are of less importance. Moreover, in the second EOF (26.6% of data variance) and third EOF (21.6% of data variance) the contribution of Quen Quen and Puerto Madryn respectively becomes important. Before one concludes that these modes of ENSO-related sea-level variability along the southwest Atlantic coast do not exist after 1980, one should first take into account that the 1958–80 partial index was constructed by using data from six stations, whereas only three stations were available for the 1981–97 partial index.

Thus, the 1958–80 index was reconstructed by using only the three stations that have data during the period 1981–97 (namely Mar de Plata, Palermo, Cananea). As in the case of 1981–97 index, all the ENSO-related signal was contained in the first EOF, which accounted for the 58.2% of the data variance. The presence of ENSO signatures in higher than the first EOF during 1958–80 only when all available tide-gauge data are used supports the speculation that the distinct modes of ENSO-related sea-level variability along the southwest Atlantic are not present after 1980 because of the unavailability of data from other tide-gauge stations.

As mentioned in a preceding paragraph, there is a significant increase in the correlation coefficient between SOI and southwest Atlantic tide-gauge data after 1980. This increase is also present in the first EOF of the data set. When the EOFs of the three stations that have data for the whole period 1958–97 are extracted, the correlation of the first EOF with SOI is −0.32 for the time span 1958–80. This correlation

increases to −0.66 after 1980. Thus ENSO signature in the region appears significantly enhanced during the last two decades. This is consistent with the increase in the intensity of El Niño events during the last 20 years (FEDOROV and PHILANDER, 2000).

CONCLUSIONS

The construction of regional sea-level indices for the investigation of interannual sea-level variability provides a robust method of examining sea-level changes in oceanic basin scales. The regional sea-level indices are consistent, major events and forcing mechanisms can be identified. Regional indices can also be used for establishing teleconnections amongst different basins and improving understanding of the ocean–atmosphere dynamics. Thus, construction of regional indices can be used in the search for evidence of climatic change. In most cases coherent regional variability is accommodated only in the first EOF of the tide-gauge data and in a few cases in the second. Low-frequency decadal sea-level variability was observed in most of the regional sea-level indices.

Sea level in the region of northwest Europe is highly driven by NAO. Sea level in this region is also positively correlated with the AO index. In the other side of the basin the signature of NAO is present in the second EOF of the data as only half of the tide gauges are within the area of immediate NAO forcing. The second EOF of northwest Atlantic was also found to be correlated with the AO index and the latitudinal position of the north wall of Gulf Stream.

ENSO is the dominant forcing mechanism in the eastern Pacific and the southwest side of the basin. Sea-level changes over these two regions are out of phase and thus negatively correlated. The high correlation between southwest Atlantic and these regions of the Pacific establishes a teleconnection between the two basins. ENSO influence on sea level in the region can be teleconnected through the PSA teleconnection pattern. The distinct modes of ENSO-related variability observed between 1957 and 1980 are not present during 1981–1997, but this is an artifact that arises because of data availability. An increase in the correlation of SOI with the southwest Atlantic index was observed after 1980. Distinct modes of sea level in the northwest and north-central parts of the Pacific do not appear to be directly influenced by ENSO. On decadal scales, strong negative correlation of the northwest Pacific sea-level index and the PDO index was observed.

The causes of the regional coherency have not been discussed. The spatial structure of atmospheric pressure and wind, as well as thermohaline changes, are probably the major contributors. Research into the causation of the spatial coherency to the sea-level signal needs to be undertaken to resolve the contribution of each of the contributing parameters. Similar analysis in the frequency domain examining the spatial coherency and the teleconnections at particular frequency bands is presently underway as part of the European Sea Level Service Research-Infrastructure project EC EVRICT-2002-40025 and will help clarify the issues identified in this paper.

ACKNOWLEDGMENTS

We thank Prof. Phil Woodworth for his critical review of the paper. We also thank Prof. Stylianos Mertikas for his support. Part of this work was funded by EC EVR1-CT-2002-40025, ESEAS-RI, and EC EVR1-CT-2001-40019, GAVDOS projects.

LITERATURE CITED

- ALLAN, R.J.; REASON, C.J.; LINDESAY, J.A., and ANSELL, T.J., 2003. Protracted ENSO episodes and their impacts in the Indian Ocean region. *Deep-Sea Research II*, 50, 2331–2347.
- ANDERSSON, H.C., 2002. Influence of long term regional and large scale atmospheric circulation on the Baltic sea level. *Tellus*, 54(A), 76–88.
- BLAHA, J. and REED, R., 1982. Fluctuations of sea level in the western North Pacific and inferred flow of the Kuroshio. *Journal of Physical Oceanography*, 12, 669–677.
- BYE, J.A.T. and GORDON, A.H., 1982. Speculated cause of inter-hemispheric oceanic oscillation. *Nature*, 296, 52–54.
- CABANES, C.; CAZENAVE, A., and LE PROVOST, C., 2001. Sea level rise during past 40 years determined from satellite and in situ observations. *Science*, 294, 840–842.
- CARLETON, A.M., 2003. Atmospheric teleconnections involving the Southern Ocean. *Journal of Geophysical Research*, 108(C4), DOI: 10.1029/2000JC000379.
- CAZENAVE, A.; DOMINH, K.; GENNERO, M.C., and FERRET, B., 1998. Global mean sea level changes observed by Topex-Poseidon and ERS-1. *Physics and Chemistry of the Earth*, 23(9–10), 1069–1075.
- CHELTON, D.B. and DAVIS, R.E., 1982. Monthly mean sea-level variability along the west coast of North America. *Journal of Physical Oceanography*, 12, 757–783.
- CHELTON, D.B. and ENFIELD, D.B., 1986. Ocean signals in tide gauge records. *Journal of Geophysical Research*, 91(B9), 9081–9098.
- CHOU, C.; TU, J.-Y., and YU, J.-Y., 2003. Interannual variability of the western North Pacific summer monsoon: differences between ENSO and non-ENSO years. *Journal of Climate*, 16, 2275–2287.
- CHURCH, J.A.; GREGORY, J.M.; HUYBRECHTS, P.; KUHN, M.; LAMBECK, K.; NHUAN, M.T.; QIN, D., and WOODWORTH, P.L., 2001. Changes in sea level. In: *Intergovernmental Panel on Climate Change Third Assessment Report*. Cambridge, UK: Cambridge University Press, pp. 639–694.
- CORTI, S.; MOLTENI, F., and PALMER, T. N., 1999. Signature of recent climate change in frequencies of natural atmospheric circulation regimes. *Nature*, 398, 799–802.
- DOUGLAS, B.C., 2001. Sea level change in the era of the recording tide gauge. In: DOUGLAS, B.C.; KEARNEY, M.S., and LEATHERMAN, S.P. (eds.), *Sea Level Rise: History and Consequences*. San Diego, California: Academic Press, pp. 37–64.
- FEDEROV, A.V. and PHILANDER, S.G., 2000. Is El Niño changing? *Science*, 288, 1997–2002.
- GARREAU, R.D. and BATTISTI, D.S., 1999. Interannual (ENSO) and interdecadal (ENSO-like) variability in the Southern Hemisphere tropospheric circulation. *Journal of Climate*, 12, 2113–2123.
- GIANNINI, A.; CHIANG, J.C.H.; CANE, M.A.; KUSHNIR, Y., and SEAGER, R., 2001. The ENSO teleconnection to the tropical Atlantic Ocean: contributions of the remote and local SSTs to rainfall variability in the tropical Americas. *Journal of Climate*, 14, 4530–4544.
- HANLEY, D.E.; BOURASSA, M.A.; O'BRIEN, J.J.; SMITH, S.R., and SPADE, E.R., 2003. A quantitative evaluation of ENSO indices. *Journal of Climate*, 16 (8), 1249–1258.
- HARE, S.R.; MANTUA, N.J., and FRANCIS, R.C., 1999. Inverse production regimes: Alaska and west coast pacific salmon. *Fisheries*, 24, 6–14.
- HOLGATE, S.J. and WOODWORTH, P.L., 2004. Evidence for enhanced coastal sea level rise during the 1990s. *Geophysical Research Letters*, 31, L07305, DOI:10.1029/2004GLO19626.
- HOREL, J.D. and WALLACE, J.M., 1981. Planetary scale atmospheric phenomena associated with the Southern Oscillation. *Monthly Weather Review*, 109, 813–829.
- HURRELL, J.W., 1995. Decadal trends in the North Atlantic Oscillation: Regional temperatures and precipitation. *Science*, 269, 676–679.
- HURRELL, J.W., 1996. Influence of variations in extratropical wintertime teleconnections on Northern Hemisphere temperature. *Geophysical Research Letters*, 23(6), 665–668.
- HWANG, C. and KAO, R., 2002. TOPEX/POSEIDON-derived space-time variations of the Kuroshio Current: applications of a gravimetric geoid and wavelet analysis. *Geophysical Journal International*, 151, 835–847.
- JANICOT, S.; TRZASKA, S., and POCCARD, I., 2001. Summer Sahel-ENSO teleconnection and decadal time scale SST variations. *Climate Dynamics*, 18, 303–320.
- JONES, P.D.; JÓNSSON, T., and WHEELER, D., 1997. Extension to the North Atlantic Oscillation using early instrumental pressure observations from Gibraltar and South-West Iceland. *International Journal of Climatology*, 17, 1433–1450.
- KAROLY, D.J., 1989. Southern hemisphere circulation features associated with El Niño–Southern Oscillation events. *Journal of Climate*, 2, 1239–1252.
- MANTUA, N.J.; HARE, S.R.; ZHANG, Y.; WALLACE, J.M., and FRANCIS, R.C., 1997. A Pacific decadal climate oscillation with impacts on salmon production. *Bulletin of the American Meteorological Society*, 78, 1069–1079.
- MILLER, L. and DOUGLAS, B.C., 2004. Mass and volume contributions to 20th century global sea level rise. *Nature*, 428, 406–409.
- MO, K.C. and HIGGINS, R.W., 1998. The Pacific–South American modes and tropical convection during the southern hemisphere winter. *Monthly Weather Review*, 126, 1581–1596.
- NEREM, R.S.; CHAMBERS, D.P.; LEULIETTE, E.W.; MITCHUM, G.T., and GIESE, B.S., 1999. Variations in global mean sea level associated with the 1997–1998 ENSO event: implications for measuring long term sea level change. *Journal of Geophysical Research*, 26(19), 3005–3008.
- OSBORN, T.J.; BRIFFA, K.R.; TETT, S.F.B.; JONES, P.D., and TRIGO, R.M., 1999. Evaluation of the North Atlantic Oscillation as simulated by a coupled climate model. *Climate Dynamics*, 15, 685–702.
- PETERSON, R.G. and WHITE, W.B., 1998. Slow oceanic teleconnections linking the Antarctic Circumpolar Wave with the tropical El Niño–Southern Oscillation. *Journal of Geophysical Research*, 103(C11), 24,573–24,583.
- PREISENDORFER, R., 1988. *Principal Component Analysis in Meteorology and Oceanography*. Amsterdam: Elsevier, 425p.
- QIU, B., 2000. Interannual variability of the Kuroshio extension system and its impact on the wintertime SST field. *Journal of Physical Oceanography*, 30, 1486–1502.
- SHENNAN, I. and WOODWORTH, P.L., 1992. A comparison of late Holocene and 20th-century sea level trends from the UK and North Sea region. *Geophysical Journal International*, 109, 96–105.
- SHINDELL, D.T.; MILLER, R.; SCHMIDT, G.A., and PANDOLFO, L., 1999. Simulation of recent northern winter climate trends by greenhouse-gas forcing. *Nature*, 399, 452–455.
- SIRVEN, J.; FRANKIGNOUL, C.; DE COETLOGON, G., and TAILLANDIER, V., 2002. On the spectrum of wind-driven baroclinic fluctuations of the ocean in the midlatitudes. *Journal of Physical Oceanography*, 32, 2405–2417.
- THOMPSON, D.W.J. and WALLACE, J.M., 1998. The arctic oscillation signature in the wintertime geopotential height and temperature fields. *Geophysical Research Letters*, 25, 1297–1300.
- TSIMPLIS, M.N. and JOSEY, S.A., 2001. Forcing of the Mediterranean Sea by atmospheric oscillations over the North Atlantic. *Geophysical Research Letters*, 28(5), 803–806.
- TSIMPLIS, M.N. and RIXEN, M., 2002. Sea level in the Mediterranean Sea: the contribution of temperature and salinity changes. *Geophysical Research Letters*, 29(23), 2136, DOI: 10.1029/2002GL015870.
- TSIMPLIS, M.N.; WOOLF, D.K.; OSBORN, T.J.; WAKELIN, S.; WOLF, J.; FLATHER, R.; SHAW, A.G.P.; WOODWORTH, P.; CHALLENGER, P.; BLACKMAN, D.; PERT, F.; YAN, Z., and JERJEVA, S., 2004. Towards

- a vulnerability assessment of the UK and northern European coasts: the role of regional climate variability. *Philosophical Transactions of the Royal Society London series A*, 363, 1329–1358.
- WAKELIN, S.L.; WOODWORTH, P.L.; FLATHER, R.A., and WILLIAMS, J.A., 2003. Sea level dependence on the NAO over the north-west European continental shelf. *Geophysical Research Letters*, 30(7), DOI:10.1029/2003GL017041.
- WALLACE, J.M., 2000. North Atlantic Oscillation/annular mode: two paradigms—one phenomenon. *Quarterly Journal of the Royal Meteorological Society*, 126, 791–805.
- WANG, B.; WU, R.X., and FU, L., 2000. Pacific-East Asian teleconnection: how does ENSO affect East Asian climate? *Journal of Climate*, 13, 1517–1536.
- WHITE, W.B. and PETERSON, R.G., 1996. An Antarctic circumpolar wave in surface pressure, wind, temperature and sea-ice extent. *Nature*, 380, 699–702.
- WOODWORTH, P.L., 1990. Toward routine global and regional sea level indices. In: EDEN, H.F. (ed.), *Toward an Integrated System for Measuring Long Term Changes in Global Sea Level*. Report of a workshop held at Woods Hole Oceanographic Institution, May, 1990. Washington DC: Joint Oceanographic Institutions Inc. (JOI), 178p. & Appendix, pp.121–131.
- WOODWORTH, P.L., 1990. A search for accelerations in records of European mean sea level. *International Journal of Climatology*, 10, 129–143.
- WOODWORTH, P.L. and PLAYER, R., 2003. The permanent service for mean sea level: an update to the 21st century. *Journal of Coastal Research*, 19(2), 287–295.
- WOODWORTH P.L.; TSIMPLIS, M.N.; FLATHER R.A., and SHENNAN, I., 1999. A review of the trends observed in British Isles mean sea level data measured by tide gauges. *Geophysical Journal International*, 136, 651–670.
- WOOLF, D.; SHAW, A., and TSIMPLIS, M.N., 2004. The influence of the North Atlantic Oscillation on sea level variability in the North Atlantic Region. *The Global Atmosphere and Ocean System*, 9(4), 145–167.
- WYRTKI, K., 1974. Equatorial currents in the Pacific 1950–1970 and their relations to the trade winds. *Journal of Physical Oceanography*, 4, 372–380.
- YAN, Z.; TSIMPLIS, M.N., and WOOLF, D., 2004. An analysis of relationship between the North Atlantic Oscillation and sea level changes in north-west Europe. *International Journal of Climatology*, 24, 743–758.
- ZHANG, Y.; WALLACE, J.M., and BATTISTI, D.S., 1997. ENSO-like interdecadal variability: 1900–93. *Journal of Climate*, 10, 1004–1020.
- ZORITA, E. and GONZÁLES-ROUO, F., 2000. Disagreement between predictions of the future behaviour of the Arctic Oscillation as simulated in two coupled models: implications for global warming. *Geophysical Research Letters*, 27, 1755–1758.

APPENDIX

One table has been prepared for each of the regional sea-level indices constructed. Each table contains the weights of each of the time series (tide-gauge station names) used in the extraction of the EOFs. The box heads of the tables contain three lines: the time span covered by the data set (first line), the associated EOF (second line), and the variance of the tide-gauge data explained by the EOFs used in the analysis (third line).

Appendix Table 1. Northeast Atlantic and North Sea Index.

| Time Span | 1932–61 First EOF | 1932–61 Second EOF | 1962–2000 First EOF | 1962–2000 Second EOF |
|---|----------------------|-----------------------|------------------------|-------------------------|
| Data Variance Explained | 58.3% | 31.2% | 55.2% | 18.67% |
| Bergen, Starvanger, Tredge | 0.61 | –0.06 | 0.50 | 0.24 |
| Hirtshalls, Esbjerg, Cuxhaven 2, Borkum, | 0.60 | –0.26 | 0.46 | 0.17 |
| Zeebrugge, Oostende | — | — | 0.45 | –0.30 |
| Lerwick, Aberdeen I, N. Shields, Immingham | 0.49 | 0.42 | 0.50 | –0.08 |
| Newlyn | 0.01 | 0.86 | 0.22 | –0.59 |
| Reykjavic | — | — | 0.15 | 0.67 |

Appendix Table 2. Northwest Atlantic Index. 'A' stands for the time series obtained after averaging data from the following stations: Boston, Woods Hole, Newport, New London, Willets Point, New York, Sandy Hook, and Philadelphia. 'B' represents the average of stations: Baltimore, Annapolis, Solomon's Island, and Washington DC.

| Time Span | 1903–11 | 1912–31 | 1912–31 | 1932–44 | 1932–44 | 1945–2000 | 1945–2000 |
|------------------------------|------------|-----------|------------|-----------|------------|-----------|------------|
| | First EOF* | First EOF | Second EOF | First EOF | Second EOF | First EOF | Second EOF |
| Data Variance Explained | 83.2% | 62.8% | 20.2% | 50.9% | 21.5% | 55.6% | 20.4% |
| Halifax | — | — | — | 0.13 | −0.27 | 0.12 | −0.45 |
| Portland | — | 0.52 | 0.19 | 0.27 | −0.37 | 0.10 | −0.45 |
| A | 0.58/0.55 | 0.50 | 0.32 | 0.31 | −0.40 | 0.25 | −0.42 |
| B | 0.60 | 0.53 | 0.23 | 0.28 | −0.29 | 0.27 | −0.33 |
| Hampton Rd | — | — | — | 0.23 | −0.49 | 0.28 | −0.29 |
| Wilmington | — | — | — | 0.31 | 0.23 | 0.33 | 0.04 |
| Charleston, Fort Pulaski | — | — | — | 0.37 | 0.22 | 0.33 | 0.12 |
| Mayport | — | — | — | 0.35 | 0.20 | 0.30 | 0.11 |
| Key West | — | 0.36 | −0.53 | 0.34 | 0.25 | 0.28 | 0.23 |
| St. Petersburg, Cedar Key II | — | — | — | — | — | 0.31 | 0.25 |
| Pensacola | — | — | — | 0.35 | 0.19 | 0.32 | 0.13 |
| Galveston | — | 0.28 | −0.72 | 0.30 | 0.25 | 0.27 | 0.24 |
| Port Isabel | — | — | — | — | — | 0.31 | 0.11 |

* EOF = empirical orthogonal function.

Appendix Table 3. Southwest Atlantic index.

| Time Span | 1958–80 | 1958–80 | 1958–80 | 1958–80 | 1981–97 |
|-------------------------|------------|------------|-----------|------------|-----------|
| | First EOF* | Second EOF | Third EOF | Fourth EOF | First EOF |
| Data Variance Explained | 37.5% | 26.6% | 21.7% | 9.6% | 64.0% |
| Puerto Madryn | −0.18 | 0.46 | 0.71 | 0.44 | — |
| Quequen | 0.02 | 0.79 | −0.29 | −0.08 | — |
| Mar Del Plata | 0.56 | 0.20 | 0.34 | −0.68 | 0.45 |
| Buenos Aires, Palermo | 0.59 | −0.27 | 0.32 | 0.32 | 0.62 |
| Cananea | 0.55 | 0.19 | −0.44 | 0.48 | 0.64 |

* EOF = empirical orthogonal function.

Appendix Table 4. Northeast Pacific Index. *A* represents the series obtained after averaging data from Vancouver, Victoria, Tofino, Neah Bay, Friday Harbor, and Seattle.

| Time Span | 1965–2000 First EOF | 1965–2000 Second EOF | 1940–64 First EOF | 1924–39 First EOF | 1924–39 Second EOF | 1910–23 First EOF | 1899–1909 First EOF* |
|---|------------------------|-------------------------|----------------------|----------------------|-----------------------|----------------------|-------------------------|
| Data Variance Explained | 67.1% | 22.8% | 70.2% | 32.8% | 45% | 86.4% | 78.1% |
| Seldovia, Cordova | 0.25 | –0.62 | — | — | — | — | — |
| Yakutat, Sitka, Juneau | 0.31 | –0.56 | 0.33 | — | — | — | — |
| Ketchikan, Prince Rupert, Queen Charlotte City, | 0.42 | –0.17 | 0.40 | –0.38 | 0.59 | — | — |
| Bella Bella, Port Hardy | — | — | — | — | 0.59 | 0.58 | 0.71 |
| <i>A</i> | 0.42 | 0.17 | 0.44 | –0.38 | — | — | — |
| Crescent City | 0.39 | 0.35 | 0.43 | — | — | — | — |
| San Francisco, Alameda | 0.41 | 0.29 | 0.44 | 0.53 | 0.45 | 0.59 | 0.71 |
| Port Saint Luis, Los Angeles, La Jolla, San Diego | 0.40 | 0.18 | 0.39 | 0.66 | 0.33 | 0.56 | — |

* EOF = empirical orthogonal function.

Appendix Table 5. Northwest Pacific Index. *A* represents the series obtained after averaging data from Kushimoto, Kainan, Waykayma, Tosa Shimizu, Komatsushima, Mozi, Hosojima, Aburatsu, and Misumi.

| Time Span | 1958–99 First EOF* | 1958–99 Second EOF |
|--|-----------------------|-----------------------|
| Data Variance Explained | 48.1% | 22.3% |
| Kushiro | 0.14 | 0.86 |
| Yokosuka, Aburatsubo, Uchiura, Shimizu Minato | 0.43 | –0.21 |
| <i>A</i> | 0.57 | 0.08 |
| Zhapo | 0.47 | 0.25 |
| Kamnen | 0.50 | –0.38 |

* EOF = empirical orthogonal function.

Appendix Table 6. North-Central Pacific index.

| Time Span | 1950–2000 First EOF* |
|-------------------------|-------------------------|
| Data Variance Explained | 77.9% |
| Johnson Island | 0.38 |
| Nawiliwily Bay | 0.52 |
| Honolulu | 0.54 |
| Kahului Harbor | 0.54 |

* EOF = empirical orthogonal function.

Appendix Table 7. Southwest Pacific index.

| Time Span | 1950–89 First EOF* | 1950–89 Second EOF |
|--------------------------------|-----------------------|-----------------------|
| Data Variance Explained | 51.2% | 22.5% |
| Newcastle III | 0.41 | 0.50 |
| Sydney Fort Denison, Camp Cove | 0.39 | 0.49 |
| Auckland II | 0.45 | –0.04 |
| Wellington II | 0.47 | –0.29 |
| Lyttelton II | 0.27 | –0.63 |
| Pago Pago | 0.41 | –0.16 |

* EOF = empirical orthogonal function.

Appendix Table 8. Southeast Pacific index.

| Time Span | 1950–91 First EOF* |
|-------------------------|-----------------------|
| Data Variance Explained | 74.6% |
| La Libertad | 0.46 |
| Arica | 0.53 |
| Antofagasta | 0.49 |
| Caldera | 0.51 |

* EOF = empirical orthogonal function.